



Cite this: *Chem. Sci.*, 2024, **15**, 8639

All publication charges for this article have been paid for by the Royal Society of Chemistry

Received 2nd February 2024  
Accepted 1st May 2024

DOI: 10.1039/d4sc00814f  
[rsc.li/chemical-science](http://rsc.li/chemical-science)

## Introduction

Photocatalysis is a powerful method to promote transformations induced by light as a source of renewable energy.<sup>1</sup> To do so, a photocatalyst is required to achieve the first activation step of the reaction. Mechanistically, the excited photocatalyst can promote either a single electron transfer (SET) or an energy transfer (EnT) to a substrate. Various applications have been developed based on this concept including water splitting,<sup>2</sup> organic synthesis,<sup>3</sup> photopolymerization,<sup>4</sup> and life-science.<sup>5</sup> Until 2019, most of the photocatalysts were developed in the UV-visible range<sup>6</sup> but these wavelengths present some drawbacks. First, the irradiation under UV-visible light can be energetic enough to provide side-reactions and selectivity issues especially when a polyfunctionalized molecule is considered.<sup>7</sup> Secondly, light penetration required for scale-up procedures or photopolymerization is higher with a longer light wavelength like near infrared (NIR) light.<sup>8</sup> Finally, the NIR-light is biocompatible since the biological tissue does not absorb NIR-photons resulting in a non-damageable irradiation (Fig. 1a).<sup>9</sup>

Two main families of NIR-photocatalysts have been developed.<sup>10</sup> Organometallic complexes such as Os-complexes,<sup>11</sup> Zn-phthalocyanines,<sup>12</sup> and Ru-polypridyl<sup>13</sup> offer a large panel of photophysical and redox properties that can be tuned by modifying the ligands. However, their preparation and

sensitivity are usually the limiting factors that prevent some potential applications. Additionally, some organometallic complexes (aluminum 2,3-naphthalocyanines,<sup>14</sup> metal-phthalocyanines,<sup>15,16</sup> bacteriochlorophyll *a*<sup>17</sup>) have been employed as photocatalysts to trigger radical photopolymerization in an efficient manner. The second family of NIR-photocatalysts is based on organic structures (Fig. 1b). In this case, redox potentials are currently rather limited, but such catalysts are accessible, stable, and non-toxic. For instance, the squaraine family drew the attention of chemists thanks to their ability to promote SET, they have been used to initiate photopolymerization by the reduction of an iodonium salt<sup>18</sup> but also to promote oxidation of amines in organic processes with Sq687.<sup>19</sup> Recently, other organic dyes such as bridged Eosin Y (BEY),<sup>20</sup> BODIPY (BDP)<sup>21</sup> and dibenzothiazole (dBIP)<sup>22</sup> have also been considered and applied for organic synthesis. The huge variety of complementary NIR-organic dyes opens new perspectives to reach interesting redox potentials and photophysical properties that can be applied in molecular and macromolecular chemistry.

To complete this collection of NIR-organic photocatalysts, cyanine derivatives are probably the most valuable candidates. Cyanines are formed by a polymethine chain with odd carbons surrounded by two heterocycles that offer an unlimited number of structures by changing and functionalizing these two parts (Fig. 1c). In this perspective, we will present the recent advances in the development of cyanine photocatalysts, a field of research that has been developed recently and showing a great potential.

Laboratoire d'Innovation Moléculaire et Applications (LIMA), UMR 7042, Université de Haute-Alsace (UHA), Université de Strasbourg, CNRS, Mulhouse, 68100, France.  
E-mail: [morgan.cormier@uha.fr](mailto:morgan.cormier@uha.fr); [jean-philippe.goddard@uha.fr](mailto:jean-philippe.goddard@uha.fr)

† Equal contribution.



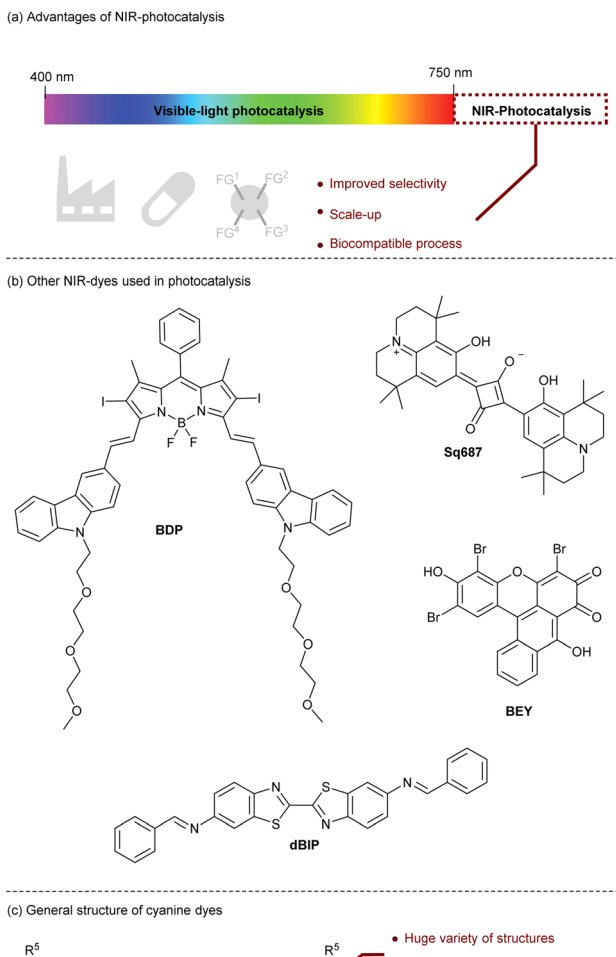


Fig. 1 Context.

## Cyanines: properties and non-catalytic applications

The cyanine family is huge and can be classified according to the chemical structures of the compounds. Among them we can cite closed chain cyanines, streptocyanines and merocyanines. They are all different in their terminal parts which can be a heterocyclic ring (symmetric or non-symmetric), a non-heterocyclic ring, an amino or carbonyl group for example. Cyanines can also be classified according to the number of methine groups present: monomethine, trimethine, pentamethine, heptamethine.<sup>23</sup> Their absorption properties are clearly influenced by the size of the polymethine chain. Indeed, adding an extra conjugated carbon–carbon double bond provides a redshift of about 100 nm in the absorption spectrum. For applications in the near-infrared domain, heptamethine cyanines are the most relevant dyes and this perspective review will be focused on this type of scaffold. Furthermore, other important photophysical properties are tunable thanks to modifications of specific parts of the cyanines (Fig. 2a).<sup>24</sup> The synthesis and

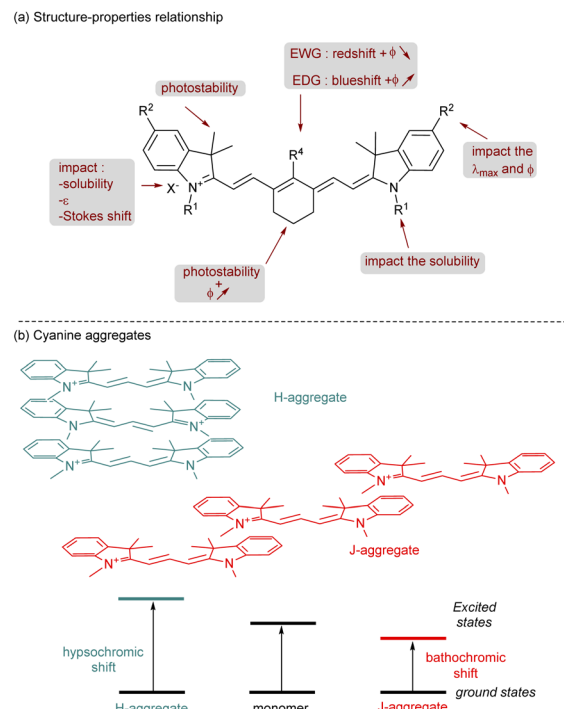


Fig. 2 Photophysical properties of cyanines.

modification of cyanines have undergone intensive investigations, empowering chemists to design a wide range of structures. This will be further explained in the dedicated section of this review. Adding cyclohexyl (or cyclopentyl) to the polymethine chain brings rigidification of the structure and prevents photoisomerization and photodegradation which slightly improve the quantum yield of fluorescence ( $\phi$ ). The photostability is also enhanced by attaching sterically congested groups in various parts of the cyanine. For instance, in indole-based cyanines, the addition of a dimethyl group at position 3 of the indolenium ring is common and efficient for this purpose. The photostability of cyanines is a crucial parameter that should be considered for their promising applications. Usually, the degradation is due to dioxygen reactive species<sup>25</sup> ( $^1\text{O}_2$  or superoxide anion) but recently it was also demonstrated that cyanines can undergo iterative phototruncations of the polymethine chain.<sup>26</sup>

Then, photophysical properties are highly customizable by changing the heterocycle or by adding a functional group on it (modification of  $R^2$ ). Since the conjugation on the  $\pi$ -system is modified the value of the  $\lambda_{\text{max}}$  and quantum yield of fluorescence is affected. Playing with functional groups at the *meso*-position ( $R^4$ ) will also change these properties. If  $R^4$  is an electron-withdrawing group (EWG) the absorption is shifted to the red part of the spectrum and the quantum yield of the fluorescence is decreasing, the opposite results are obtained with electron-donating groups (EDG). The nature of the counter anion is also important, classically halide, perchlorate, hexafluorophosphate, nitrate or tetrafluoroborate are selected. The counter anion affects the charge distribution which impacts the



$\varepsilon$  and the Stokes shift. Moreover, it plays a crucial role in cyanine solubility.<sup>27</sup>

This parameter is also tunable through the modification of  $R^1$  attached to the nitrogen of the heterocycle. Chemists were mainly focused on the solubility of cyanines in water for various applications and to do so, adding a sulfonate or a carboxylate is a determining factor to reach this goal. This modification is also crucial to avoid aggregate formation in solution (especially in water). Indeed, in solution cyanines are able to form, by self-association, supramolecular structures known as H-aggregates or J-aggregates (Fig. 2b).<sup>28</sup> An H-aggregate is obtained when the structure is parallel to form a sandwich-type arrangement. The head-to-tail organization of these dyes is called the J-aggregate. The H-aggregate involves a hypsochromic shift in absorption whereas the corresponding J-aggregate gives a bathochromic shift and a narrow Stokes shift. Quantum yields are substantially impacted by the formation of aggregates, and most of the time H-aggregates are unable to reach high values of  $\phi$ . Except for specific applications with J-aggregates,<sup>29</sup> usually these conditions are chosen to inhibit the formation of aggregates.

In addition to their photophysical properties, cyanines possess interesting redox properties from their ground states and excited states. However, the structure–redox property relationship is less commented in the literature.<sup>30</sup> It was proved that extending the polymethine chain increases the  $E_{1/2}^{\text{ox}}$  and decreases the  $E_{1/2}^{\text{red}}$ . The effect of donor–acceptor properties of functional groups attached to the cyanine is important but not often regular. Nonetheless, the impact of counter-anions on redox properties is less pronounced.

Thanks to these remarkable properties, heptamethine cyanines have been used for many applications (Fig. 3). Their fluorescence properties and biocompatibility are currently used for daily analysis as biosensors (pH, ROS, thiols,  $\text{H}_2\text{O}_2$ ...), for bioimaging or even for drug delivery by photocaging.<sup>31</sup> For all these applications, a modification of the *meso* position is required to attach a functional group used for the biomolecule recognition.

In addition to the fluorescence, cyanines present other interesting features in the excited state that are useful for various applications. They are able to convert light energy into thermal energy through a non-radiative process, this property is applied to photothermal therapy (PTT).<sup>32</sup> Even more interestingly, cyanines can promote energy transfer (EnT) from their triplet state to photosensitize  $^3\text{O}_2$  into  $^1\text{O}_2$ . This photosensitizer character is applied for photodynamic therapy (PDT).<sup>33</sup> To reach

the best quantum yields of  $^1\text{O}_2$ , simple modifications of the cyanine can be done to favor inter-system crossing (ISC) such as the introduction of heavy atoms (iodine,<sup>34</sup> selenium<sup>35</sup>), anthracene<sup>36</sup> or paramagnetic scaffolds.<sup>37</sup> Cyanines are also well-known for their applications in solar-cells as photosensitizers.<sup>38</sup> Their ability to transfer an electron *via* a SET process from their excited state is useful in Dye-Sensitized Solar Cells (DSSCs) but this property could also be employed in photocatalytic reactions.

**Synthesis of cyanine dyes.** The first historical cyanine synthesis was described by C. H. Greville Williams in 1856.<sup>39</sup> This synthesis follows a condensation between two quaternary quinolinium salts **1** and **2**, under basic conditions, to afford the first cyanine **3** as a blue-coloured dye (Scheme 1).

During the 19th century, newly discovered dyes were often quickly applied in the textile industry as dyeing agents. Unfortunately, the first cyanine **3** was not useful for the dyeing industry due to its low photostability.<sup>40</sup> To improve this parameter, other cyanines have been developed through different synthetic routes. For decades, different trimethine, tetramethine, and pentamethine cyanine dyes were synthesized.<sup>41</sup> In this section dedicated to cyanine synthesis, heptamethine cyanine dyes (seven carbons on the central chain) will be highlighted according to their absorption in the near infrared window and their application in photocatalysis. The first classical synthesis of heptamethine dyes involves two key substrates: a quaternary indolenium **8** and a modified Schiff base **10** (Scheme 2).

To obtain the quaternary indolenium moiety **8**, the strategy starts with a Fischer indole type synthesis from the phenylhydrazine hydrochlorate salt **4** and a ketone. The 3-methylbutan-2-one **5** is often used to improve the stability of the cyanine by increasing the steric hindrance. Then, the alkyl iodide **7** is substituted by the indole **6** to quaternize the indolenine nitrogen and afford the indolenium **8**. The modified Schiff base **10** was obtained through a Vilsmeier–Haack formylation, starting from a cyclohexenyl derivative **9**. At the end, a condensation between **8** and **10**, with a ratio 2 : 1, under basic conditions, gives the corresponding cyanine dye with 70% yield for the reported example. This approach is reasonably general and by modifications of different building blocks several cyanines can be prepared in moderate to excellent yields.

Even more interesting, by modification of the key intermediates, unsymmetrical cyanine dyes have been obtained.<sup>42</sup> Indeed, this synthesis route was applied with two different quaternary indolenium moieties condensed on a Schiff base derivative to obtain unsymmetrical dyes. This strategy was pushed further with a microwave assisted solid-phase synthesis,

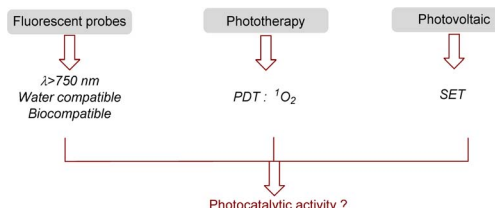
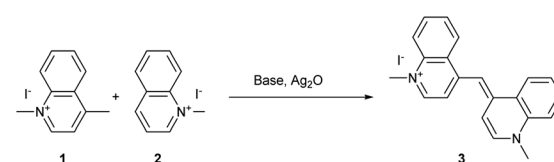
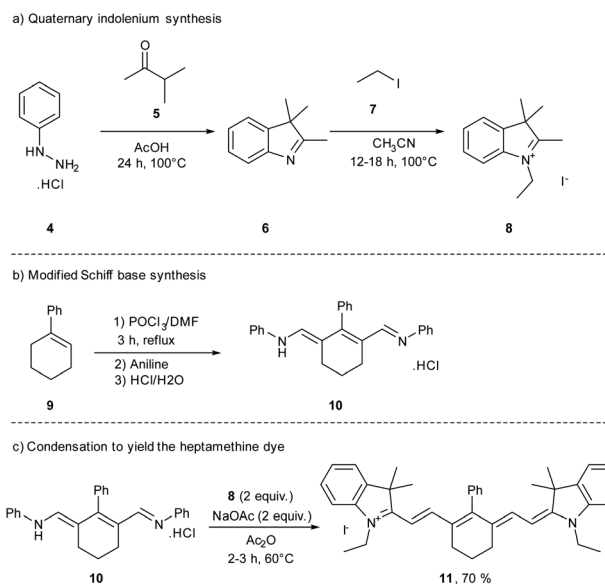


Fig. 3 Main applications of NIR-cyanine dyes.

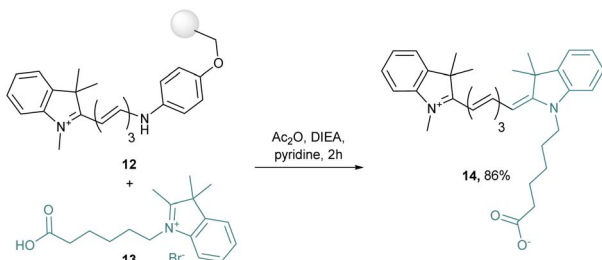


Scheme 1 First cyanine dye synthesis described by Greville Williams.





Scheme 2 Classical synthesis route toward heptamethine dyes.



Scheme 3 Heterogeneous unsymmetrical cyanine synthesis.

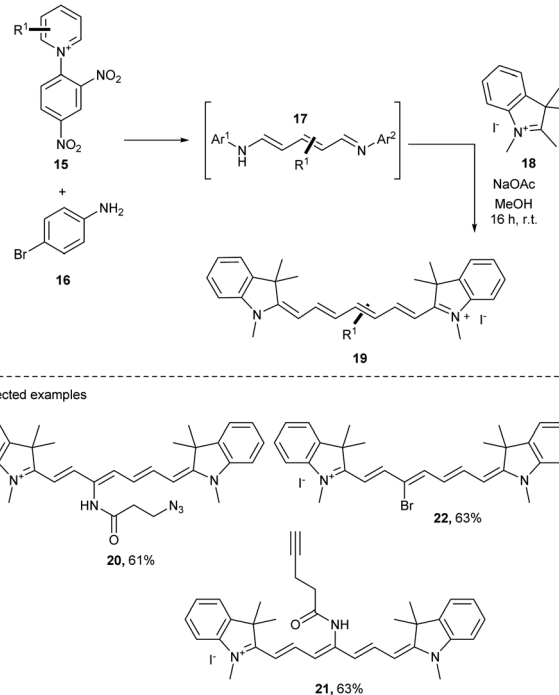
in which a resin-bound hemicyanine **12** is prepared by addition under microwave conditions of indolenium into a grafted Schiff base. Then **12** is released after reaction with a quaternary ammonium salt **13** to afford the unsymmetrical cyanine **14** in 86% yield (Scheme 3).<sup>43</sup>

This strategy has been extended to many different cyanines and takes advantage of the solid-support since only one purification in the final step is required.

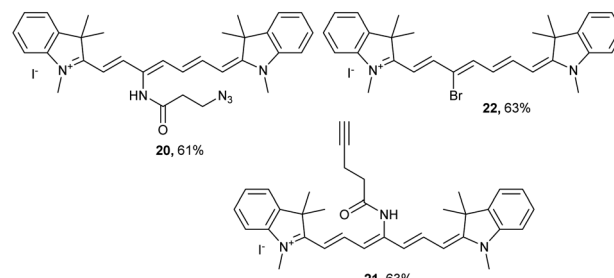
Another route of heptamethine synthesis was then developed by the group of Klán in 2019 (ref. 44) using a modification of the classical Zincke reaction.<sup>45</sup> The authors reported the use of an open form of the pyridinium salt **15** (also called the Zincke salt) obtained by substitution of two equivalents of the *p*-bromoaniline **16**. The resulting intermediate **17** was then reacted with quaternary indolenium moieties **18** under mild conditions giving the heptamethine dyes with good yields (up to 90%) with high purity after simple precipitation in ether (Scheme 4a).

This strategy is versatile and offers a large diversification of the heptamethine dyes. For instance, cyanine dyes bearing interesting functional groups on the heptamethine scaffold like azide (**20**), terminal alkyne (**21**), and bromide (**22**) were prepared in 61%, 63% and 63% yields respectively (Scheme 4b). This strategy opens the door to direct modifications of the

## (a) Zincke synthesis : strategy and conditions



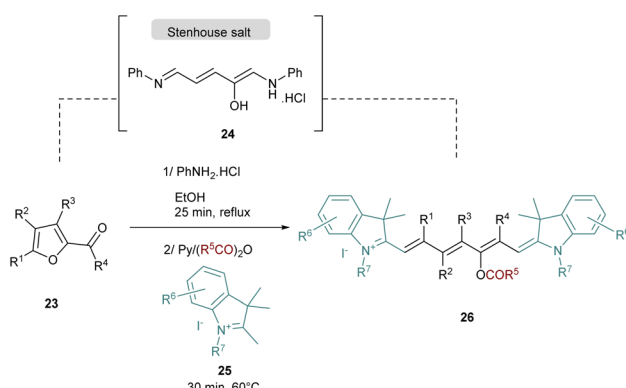
## (b) Selected examples



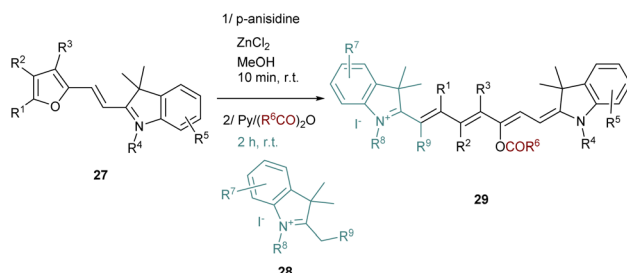
Scheme 4 The Zincke route strategy.

conjugated chain of cyanines to tune their properties or even to attach a linker which is useful for many applications. A new update has been achieved in the pyridinium strategy to prepare cyanines with a huge diversity of structures using pyridinium benzoxazole (PyBox). This pyridinium is well tolerant to various functional groups offering original substituted cyanines.<sup>46</sup>

Recently, a novel synthesis of cyanines was published by the group of Mo and the strategy is based on the one-pot preparation of a Stenhouse salt intermediate from the corresponding furfural **23** (Scheme 5).<sup>47</sup> The Stenhouse salt **24** is generated *in situ* by the addition of aniline into the furfural derivatives. This intermediate is placed under reflux and basic conditions with quaternary indolenium **25** to yield the symmetrical cyanines **26** which contain various functional groups in the polymethine chain.



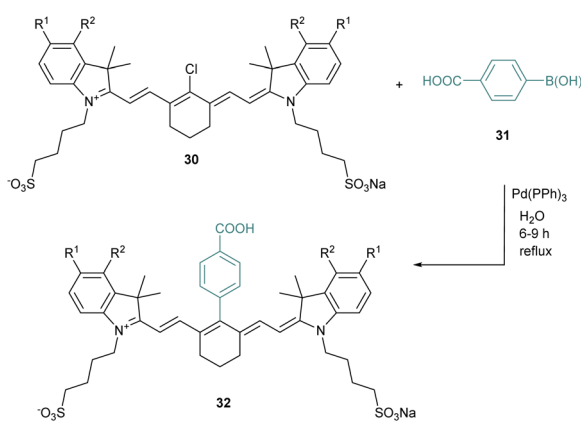
Scheme 5 One-pot strategy to yield cyanine dyes via Stenhouse salt.



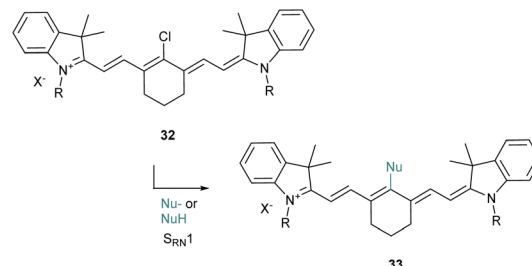
Scheme 6 Unsymmetrical dyes obtained through the one-pot strategy.

It should be noted that this strategy requires the evaporation of the ethanol after the Stenhouse salt formation to avoid the cyclization and the formation of the corresponding cyclopentenone. The synthesis of unsymmetrical cyanine dyes following this strategy was also reported after a slight modification of the procedure. The key intermediate 27 to obtain unsymmetrical dyes is a “half-cyanine” bearing a furan moiety which is stable at room temperature and easy to isolate (Scheme 6). The furan containing precursor 27 is then opened using zinc chloride and *p*-anisidine. The corresponding intermediate in this reaction is a half Stenhouse salt which is directly involved in the condensation with a second different quaternary indolenium 28. This strategy allows access to unsymmetrical heptamethine cyanines 29 with a shorter reaction time and with a high degree of functionalization.

The *meso* position is crucial to tune the properties of cyanines, and several methods have been investigated to modify it. For instance, Suzuki–Miyaura coupling reactions were described to be efficient in this specific position for different halogenated cyanines (Scheme 7).<sup>48</sup> Thus, chlorocyanines 30 react in water with the boronic acid 31 in the presence of a catalytic amount of  $\text{Pd}(\text{Ph}_3)_4$  to reach the arylated cyanine 32. This *meso*-chlorine atom substitution creates a new robust C–C bond under environment-friendly aqueous conditions with good yields (68–83%). The cross-coupling strategy is rather general and other conditions are compatible such as Heck, Sonogashira or Stille cross-coupling reactions.<sup>49</sup>



Scheme 7 Suzuki–Miyaura coupling on heptamethine dyes.

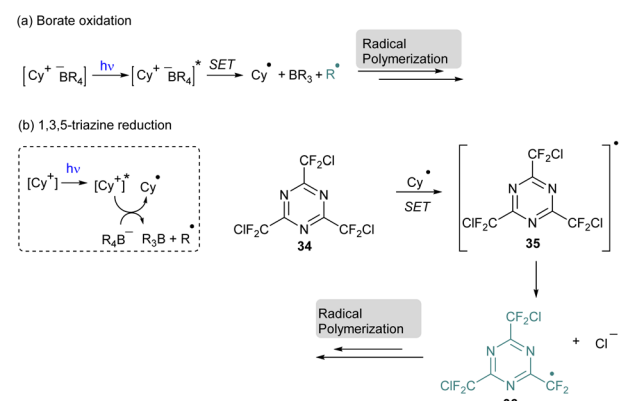


Scheme 8  $\text{SRN1}$  pathway for heptamethine diversification.

The halogenated heptamethine at the *meso* position can also be substituted by nucleophiles as proposed originally by the group of Strekowski for the introduction of alcoholates and thiolates (Scheme 8).<sup>50</sup> They reported that the substitution would probably follow an  $\text{SRN1}$  (substitution radical nucleophilic unimolecular) pathway which was proved by EPR experiments. This strategy was then applied to various nucleophiles<sup>51</sup> including alkyl amines,<sup>52</sup> azides,<sup>53</sup> selenols<sup>54</sup> or acetylacetone (acac).<sup>55</sup> This approach is versatile and generally provides an interesting tool to quickly tune the properties of cyanine derivatives.

### Cyanines as NIR-photocatalysts

**Application in photopolymerization.** Compared to previous methods of polymerization, involving high-temperature heating,<sup>56</sup> the emergence of photopolymerization made the process simpler to operate reducing the amount of energy compared to the thermal process.<sup>57</sup> In addition, this technique enables a spatial and temporal control of the polymerization which found many applications in coatings, adhesives, paints, printing inks, dental restorative formulations, electronic circuits and composite materials. The photopolymerization is usually performed under UV-light irradiation allowing the generation of radical species by direct homolytic cleavage of weak bonds. However, this range of wavelengths is known to be noxious for the operator and the penetration of UV-light in chemical media is very limited. To circumvent these drawbacks, one solution consists in shifting the irradiation to near-infrared



Scheme 9 Visible-light photopolymerization with cyanine: (a) borate oxidation; (b) 1,3,5 triazine reduction.



light. To do so, a photosensitizer is needed to convert the NIR-light energy into chemical energy to trigger the initiation step.

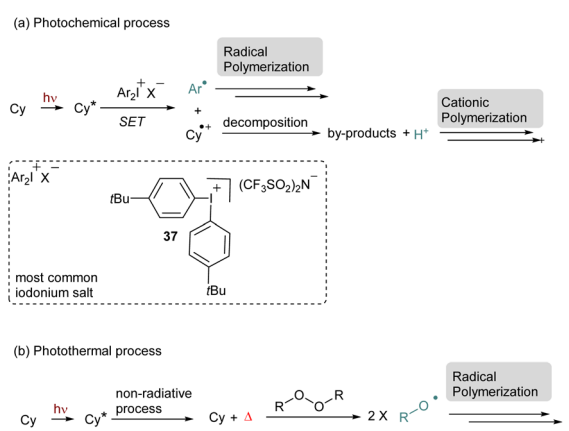
Among the NIR-photosensitizers,<sup>58,59</sup> cyanines have been intensively employed but, originally, they were used for photopolymerization with visible light. In this case, the radical polymerization occurs through the oxidation of the borate salt which is generally the counter anion of the cyanine (Scheme 9a).<sup>60</sup> In the excited state the cyanine can oxidize the borate through a Single Electron Transfer (SET) to produce the first radical species able to initiate the polymerization. This system was also extended to the reduction of 2,4,6-tris(chlorodifluoromethyl)-1,3,5-triazine **34** in a three-component system with borate to achieve under visible light conditions the first step of the radical photopolymerization (Scheme 9b).<sup>61</sup>

Then, with the development of NIR sources of irradiation, these interesting tools were adapted to be used in this corresponding window. The polymerization triggered by NIR-cyanine dyes proceeds through different pathways. The initiation step can occur *via* a SET process from the excited state of the cyanine to generate a radical species (Scheme 10a).<sup>62,59a-f</sup> In this case iodonium salts are the most employed radical initiators. A specific design of this cationic species has been achieved and usually the iodonium **37** bearing a *p*-tertbutyl group is commonly used. The effect of the counteranion is also very important especially to solve solubility issues. After the first step, the reduction of the iodonium salt, the aryl radical species can initiate radical polymerization. Additionally, this photocatalytic system is compatible with phosphines, this additive prevents polymerization inhibition of acrylates due to oxygen. Another possible pathway is to use the intermediate radical species derived from the cyanine as a source of proton. In this case, after the first SET with an iodonium salt the cyanine intermediate undergoes decomposition to provide a proton able to trigger a cationic polymerization. The release of the proton was monitored by UV-vis analyses with rhodamine B. Cyanines are also known to produce heat through a non-radiative process from their excited state. This phenomenon increases the reaction media temperature and can activate a thermal initiator, which in turn can enable the polymerization (Scheme 10b). For instance, cyanines in combination with peroxides result in the

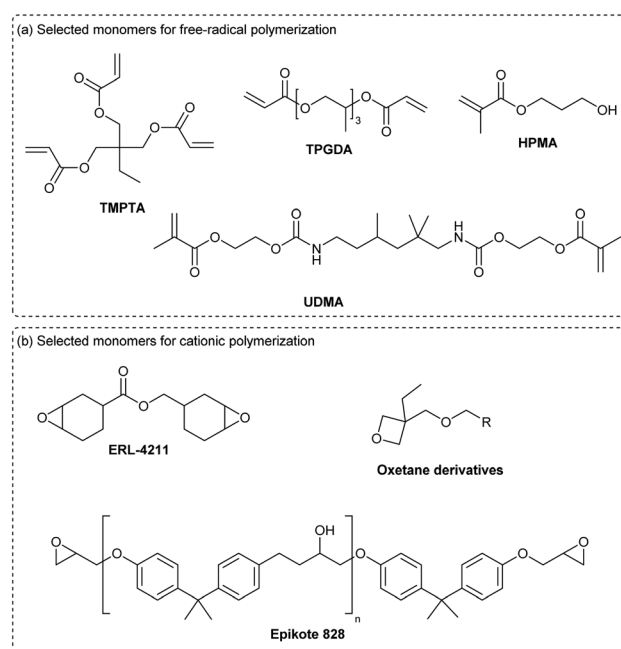
photothermal radical polymerization of acrylates or methacrylate.<sup>63</sup> Apart from peroxide, thermal initiators, such as alkoxyamine or azo derivatives, are also efficient for this purpose. Recently, the photothermal process has been applied to iodonium salts in combination with electron donating anilines. In this case a Charge Transfer Complex (CTC) is formed *in situ*, which allows the formation of an aryl radical and a subsequent free-radical polymerization after photothermal activation.<sup>59g</sup> For all of them, the temperature increase is tunable and depends on the concentration of the dye and the light power. It is often discussed that a photoredox and a photothermal process occur simultaneously which reinforced the efficiency of cyanines as photosensitizers. For instance, a combination of these two processes allows the formation of interpenetrating polymer networks (IPNs).<sup>59e,f</sup>

The photoinitiation driven by cyanines and NIR-light has proved to be compatible with classical monomers used in regular UV-vis photopolymerization (Scheme 11a). For the free-radical polymerization, acrylates, such as TMPTA (trimethylolpropane triacrylate) or TPGDA (tri(propylene glycol) diacrylate) and methacrylates like HPMA (hydroxypropyl methacrylate) or UDMA (urethane dimethacrylate) are often considered for this application. However, epoxides (ERL-4211, Epikote 828) or oxetanes are mainly employed in cationic polymerization.

Among the huge number of accessible cyanines available, photopolymerization is often achieved by commercial ones. The group of Strehmel has provided many photophysical and redox data for the most efficient cyanines.<sup>59d</sup> Interestingly, the structures of the best photosensitizers are relatively different. A selection of cyanines that are efficient for radical and cationic polymerization are presented below: **Cy791**, **Cy746**, **Cy794**, **Cy854** (Fig. 4).



Scheme 10 General mechanism of NIR-polymerization with cyanines.



Scheme 11 Selected examples of monomers compatible with cyanine-based NIR photopolymerization.



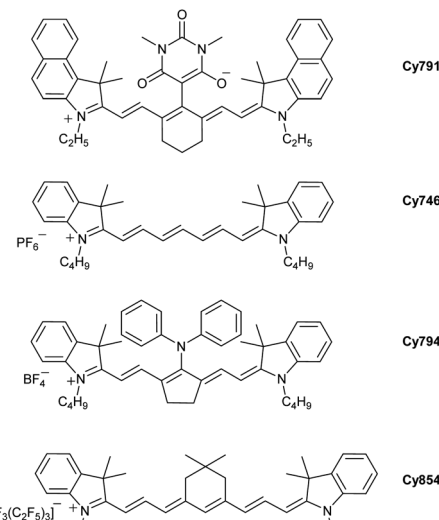
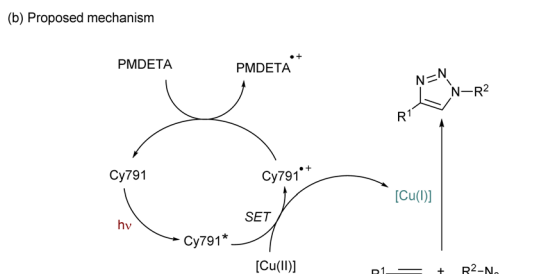
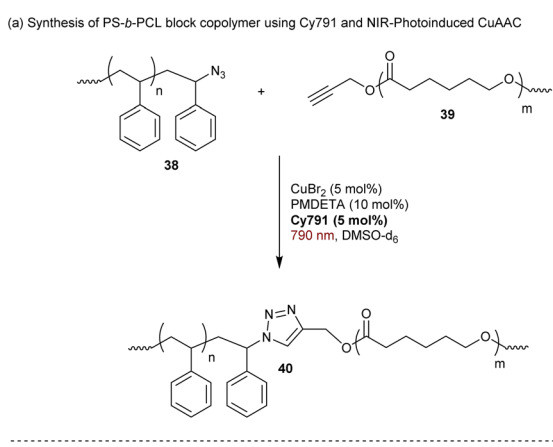


Fig. 4 Examples of cyanines used as photosensitizers.

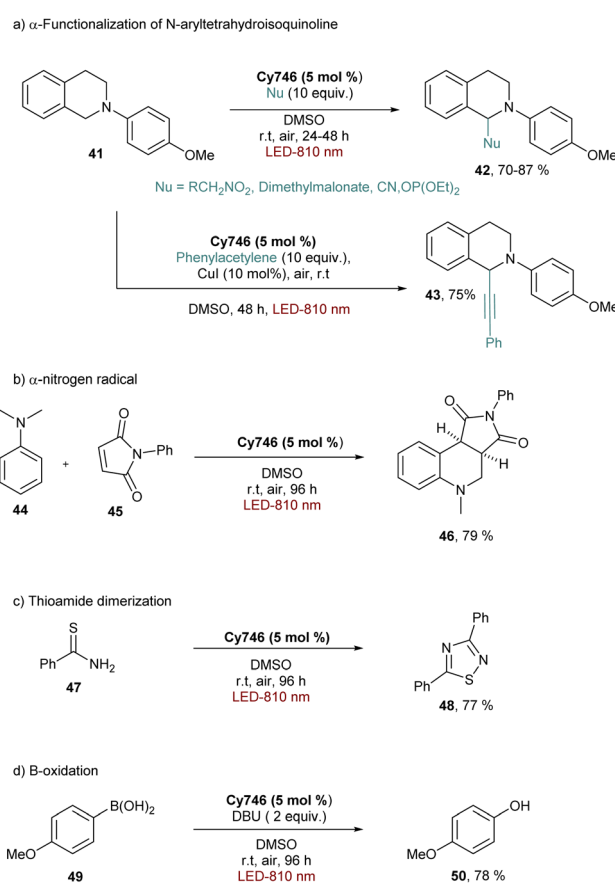
Still in the context of polymer chemistry, Strehmel and Yagci reported a cyanine-based NIR-photoinduced Copper-catalyzed Azide-Alkyne Cycloaddition click reaction (CuAAC).<sup>64</sup> This approach has been employed to prepare bloc copolymers such as polystyrene- $\beta$ -poly( $\epsilon$ -caprolactone) (PS- $\beta$ -PCL) **40** (Scheme 11a). Mechanistically, CuAAC requires a Cu(i) catalyst to achieve the cycloaddition under mild conditions. However, Cu(i) salts are sensitive to air and several solutions have been used to reduce stable Cu(ii)-complexes *in situ* to Cu(i)-complexes. The

cyanine **Cy791** bearing a barbiturate group in the *meso* position was found to be efficient for NIR-photoreduction of CuBr<sub>2</sub> to promote the CuAAC (Scheme 11b).<sup>65</sup> In order to regenerate the initial state of the cyanine after the first SET, *N,N,N',N'',N''*-pentamethyldiethylenetriamine (PMDETA) is added in the solution as a co-reductant (Scheme 12).

**Cyanine-based NIR-photocatalysis for organic synthesis.** In the course of developing NIR-photocatalysis for organic reactions, our group was the first to consider NIR-dyes as photocatalysts, specifically cyanines. A first generation of cyanines was investigated for this purpose and **Cy746** was revealed to be the best for both oxidation and reduction upon NIR-light activation.<sup>66</sup> For instance, **Cy746** is an efficient photocatalyst to obtain functionalized tetrahydroisoquinolines **41** *via* aza-Henry type reactions with nitroalkanes but also with various nucleophiles including malonate, cyanide and phosphite (Scheme 13a). The optimized conditions are also compatible with dual catalysis with copper to obtain the alkynylated product **43** in 75% isolated yield. Other oxidations have also been reported with this photocatalyst with good yields such as the cyclization of the aniline **44** with the maleimide **45** (Scheme 13b), the dimerization of the thioamide **47** (Scheme 13c) and the oxidation of the boronic acid **49** (Scheme 13d). For oxidative processes, the estimated redox potential for **Cy746** is about 0.80 V in the excited state which allows the SET mechanism with



Scheme 11 Copper-catalyzed alkyne–azide cycloaddition under NIR light using Cy791.



Scheme 13 Oxidation performed with Cy746, the first generation of cyanine-based NIR-photocatalysts.

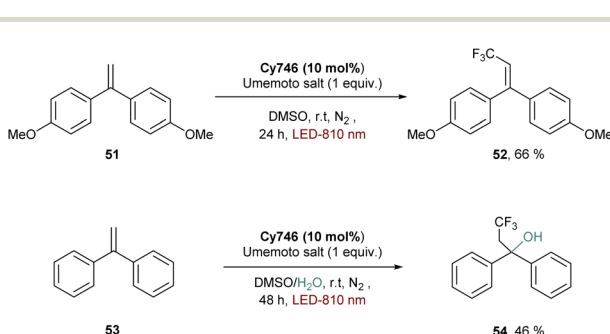
some substrates. EnT was also proved to be an alternative pathway in some oxidative processes with  ${}^1\text{O}_2$  as the oxidant. For many reactions, the competition between these two mechanisms is often observed with visible light photocatalysts.<sup>67</sup> In the case of cyanines, the same observation has been notified. For instance, **Cy746** is able to directly oxidize amines *via* the SET mechanism and form the radical cation, as it was proved by Stern–Volmer quenching experiments.<sup>66</sup> On the other hand, **Cy746** is also known as a photosensitizer to generate  ${}^1\text{O}_2$  and promote transformations with this reactive oxygen species (see the dedicated part of this perspective). At the end, both mechanisms afford similar intermediates (in the case of amine oxidation, the radical cation and iminium) making the determination of their relative contribution very challenging.

Reduction of substrates can also take place, as exemplified by the reduction of the Umemoto salt to form the trifluoromethylated alkene **52** (Scheme 14). In this case, the mechanism involves a SET between the cyanine and the sulfonylum to provide the trifluoromethyl radical which is trapped by a radical acceptor. The reaction is compatible in water media since adding  $\text{H}_2\text{O}$  as a co-solvent and nucleophile provided the hydroxyltrifluoromethylated adduct **54**.

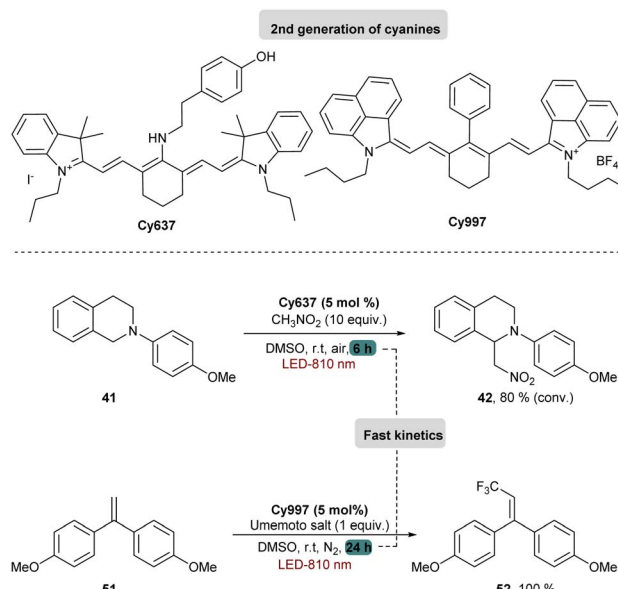
Cy746 proved its versatility and synthetic utility, however, one major issue is the slow kinetics of the mentioned reactions. To improve this aspect, a second generation of cyanine dyes was described.<sup>68</sup> A range of cyanines were synthesized and fully characterized with the estimation of their redox potentials in the excited state. They were tested in the aza-Henry and the trifluoromethylation reactions. Concerning the oxidation of tetrahydroisoquinolines, a secondary amino group on the *meso* position of the heptamethine chain was able to accelerate kinetics of different reactions (Scheme 15).

These cyanines, which have the lowest  $E_{\text{red}}^*$  values (0.68–075 V), allow conversion rates greater than 50% after only 6 h of reaction. The best result was obtained with **Cy637** in converting **41** in 80% after only 6 h compared to the 24 h needed with **Cy746**. However, comparing all cyanines did not allow demonstration of the obvious correlation between their redox potential in the excited state and the rate of the aza-Henry reaction. This can again suggest competitive mechanisms between SET and EnT.

Looking at the trifluoromethylation kinetics of **51**, a plateau is generally reached after 4 h of reaction, suggesting a possible degradation of the photocatalyst by non-selective



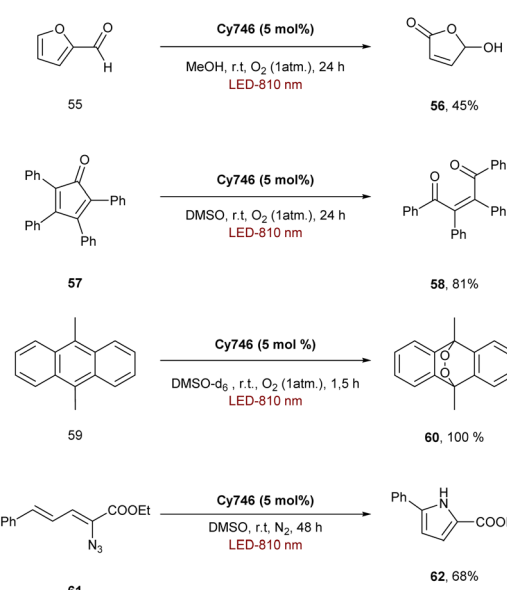
**Scheme 14** Reduction of the Umemoto salt with Cy746.



**Scheme 15** Improvement of kinetic rates with the second generation of cyanines

trifluoromethylation of the cyanine. The best results were obtained with **Cy997** (Scheme 15) which was among the fastest at the beginning of the reaction, and more importantly was the only one to achieve full conversion after 24 h. Its stability was a key parameter for efficient and rapid conversion, despite the low potential of this cyanine ( $-0.38$  V). **Cy997** also proved its efficiency in giving the trifluoromethylated product under irradiation at lower energy 940 nm (with 83% yield instead of 100% at 810 nm).

The ability of cyanines to process *via* an EnT mechanism was also explored for organic transformations. Indeed, Cy746 can also



**Scheme 16** Photosensitization transformations performed within Cv746.

Table 1 Redox properties of relevant cyanine-based photocatalysts and comparison with other organic NIR-PCat

PCat	$\lambda_{\max}^a$ (nm)	$E_{\text{red}/\text{ox}}$ vs. SCE <sup>b</sup> (V)		$E_{\text{red}/\text{ox}}^*$ vs. SCE <sup>c</sup> (V)	
		$E_{\text{ox}}$	$E_{\text{red}}$	$E_{\text{ox}}^*$	$E_{\text{red}}^*$
Cy637 <sup>68</sup>	637	0.38	-0.85	-1.19	0.72
Cy746 <sup>68</sup>	746	0.61	-0.68	-0.88	0.80
Cy791 <sup>68</sup>	791	0.41	-0.93	-1.00	0.48
Cy794 <sup>68</sup>	794	0.58	-0.64	-0.80	0.74
Cy854 <sup>59d</sup>	854 <sup>d</sup>	0.46 <sup>e</sup>	-0.33 <sup>e</sup>	n.d	n.d
Cy997 <sup>68</sup>	997	0.68	-0.27	-0.38	0.79
Sq687 <sup>19</sup>	687	0.23	-0.43	-1.45	1.22
BEY <sup>20</sup>	731	1.16	-0.34	-0.81	1.63
Methylene blue (MB) <sup>3d</sup>	664 <sup>f</sup>	1.13 <sup>g</sup>	-0.30 <sup>g</sup>	-0.68	1.60

<sup>a</sup> In DMSO. <sup>b</sup>  $E_{\text{red}/\text{ox}}$  was measured by cyclic voltammetry (CV) with respect to KCl (3 M)/Ag/AgCl reference electrode and corrected vs. SCE. The solvent was DMSO. <sup>c</sup>  $E_{\text{red}/\text{ox}}^*$  was calculated according to the Rehm-Weller equation. <sup>d</sup> In acetonitrile. <sup>e</sup>  $E_{\text{red}/\text{ox}}$  was measured by cyclic voltammetry (CV) with respect to an Ag/AgCl reference electrode in CH<sub>3</sub>CN. <sup>f</sup> In MeCN/H<sub>2</sub>O (4 : 1). <sup>g</sup>  $E_{\text{red}/\text{ox}}$  was measured by cyclic voltammetry (CV) with respect to Ag/AgCl and referenced to SCE in DCM.

perform the photosensitization of oxygen to generate  $^1\text{O}_2$  and oxidize the furfural 55 in 45% yield, the tetraphenylcyclopentadienone 57 (81% yield) and the 9,10-dimethylanthracene 59 to form the endoperoxide **60** quantitatively (Scheme 16).<sup>61,62</sup> Cy746 is highly adaptable and can also promote the photosensitization of the vinyl azide **61** to obtain, after formation of a nitrene *in situ*, the disubstituted pyrrole **62** in 68% isolated yield.

**Summary of redox properties for selected cyanine-based photocatalysts.** In this section, the redox properties of the most relevant cyanine-based photocatalysts are reported as well as the  $\lambda_{\max}$  for absorption (Table 1). In their excited state the cyanine bearing an electron donating amino group at the *meso* position presents the most negative  $E_{\text{ox}}^*$  value (-1.19 V vs. SCE) which is still far from that of Sq637 ( $E_{\text{ox}}^* = -1.45$  V vs. SCE). For the other cyanines,  $E_{\text{ox}}^*$  is between -0.80 and -1.00 V vs. SCE, consistent with other PCat in the same range of wavelengths of absorption (BEY and MB). Surprisingly, Cy997, while producing optimal results in the Umemoto salt reduction, exhibits the least negative potential in the excited state ( $E_{\text{ox}}^* = -0.38$  V vs. SCE). This outcome confirms that the redox potential alone cannot be regarded as the unique parameter in optimizing the photocatalyst. In this case, the stability of sensitive NIR-dyes is also very crucial. Interestingly, the  $E_{\text{red}}^*$  seems to be less impacted by the cyanine structure since very similar values have been determined (0.70 to 0.8 V) for these selected cyanines. Except for Cy854 (not determined in the literature), the current cyanine photocatalysts present limited  $E_{\text{red}}^*$  compared to other organic NIR-PCat. Indeed, Sq637, BEY and MB seem to be more powerful oxidants in the excited state ( $E_{\text{red}}^* > 1.20$  V), providing a perspective of amelioration for the design of new cyanine-based photocatalysts.

## Conclusions and perspectives

In conclusion, NIR-photocatalysis is only in its launching sequence. Currently, the main applications of NIR-photocatalysts are devoted to radical and cationic

photopolymerization which combine SET and photothermal processes. The application in organic synthesis is promising as it was demonstrated with a first generation of cyanine (Cy746) in oxidation, reduction and photosensitization. Then an updated and optimized version was reported with Cy637 and Cy997 which provides efficient and fast reactions in the oxidation of tetrahydroisoquinolines and reduction of the Umemoto salt.

Due to the benefits of the NIR photocatalysis compared to visible light and the potential applications of this field of research, the photochemistry driven by cyanines will play a key role in the future. However, to enrich the toolbox of cyanine photocatalysts, there are still some questions that need to be solved. First, the rationalization of the structure–photocatalytic activity relationship is required to accelerate the design of this family of photocatalysts. This is particularly interesting, to reach higher  $E_{\text{ox}}^*$  which is currently limited to 0.80 V for most of the cyanines. Concerning the energy transfer (EnT), the application is currently mainly restricted to  $^1\text{O}_2$  generation and the design of cyanines with high triplet energy would open the door to a new class of reactions triggered by NIR-light. Currently the NIR-light used either for the SET or EnT process is around 800 nm, and the highest wavelength irradiation has been achieved at 940 nm for the reduction of the Umemoto reagent with Cy997. Would it be possible to shift the light irradiation to very low energetic wavelengths (>1000 nm)? Finally, the stability of cyanines is still a challenge to achieve a more efficient process. Although some modifications on cyanines have been done to protect the heptamethine chain, these conjugated molecules remain sensitive to radical species generated in the photocatalytic process. Thus, the ideal cyanine-based photocatalyst will combine all these parameters in one structure and the future developments will tend towards its design.

## Author contributions

N. S, J. F, M. C. and J.-P. G. conceptualized, wrote and edited the perspective.

## Conflicts of interest

There are no conflicts to declare.

## Acknowledgements

The authors thank the Université de Haute-Alsace (UHA) for providing facilities and funding.

## Notes and references

- 1 R. C. McAtee, E. J. McClainand and C. R. J. Stephenson, *Trends Chem.*, 2019, **1**, 111.
- 2 (a) S. Nishioka, F. E. Osterloh, X. Wang, T. E. Mallouk and K. Maeda, *Nat. Rev. Methods Primers*, 2023, **3**, 42; (b) K. Villa, J.-R. Galán-Mascarós, N. López and E. Palomares, *Sustainable Energy Fuels*, 2021, **5**, 4560; (c) K. Maeda and K. Domen, *J. Phys. Chem. Lett.*, 2010, **1**, 2655.
- 3 (a) M. S. Kwon and Y. Lee, *Eur. J. Org. Chem.*, 2020, 6028; (b) J.-P. Goddard, C. Ollivier and L. Fensterbank, *Acc. Chem. Res.*, 2016, **49**, 1924; (c) M. H. Shaw, J. Twiltonand and D. W. C. MacMillan, *J. Org. Chem.*, 2016, **81**, 6898; (d) N. A. Romero and D. A. Nicewicz, *Chem. Rev.*, 2016, **116**, 10075; (e) R. A. Angnes, Z. Li, C. R. D. Correia and G. B. Hammond, *Org. Biomol. Chem.*, 2015, **13**, 9152; (f) C. K. Prier, D. A. Rankic and D. W. C. MacMillan, *Chem. Rev.*, 2013, **113**, 5322.
- 4 (a) V. Ferraro, C. R. Adam, A. Vranic and S. Bräse, *Adv. Funct. Mater.*, 2024, **34**, 2302157; (b) C. Wu, N. Corrigan, C.-H. Lim, W. Liu, G. Miyake and C. Boyer, *Chem. Rev.*, 2022, **122**, 5476; (c) N. Zivic, M. Bouzrati-Zerelli, A. Kermagoret, F. Dumur, J.-P. Fouassier, D. Gigmes and J. Lalevée, *ChemCatChem*, 2016, **8**, 1617.
- 5 L. Candish, K. D. Collins, G. C. Cook, J. J. Douglas, A. Gómez-Suárez, A. Jolit and S. Keess, *Chem. Rev.*, 2022, **122**, 2907.
- 6 (a) D. Ravetz, A. B. Pun, E. M. Churchill, D. N. Congreve, T. Rovis and L. M. Campos, *Nature*, 2019, **565**, 343; (b) M. Freitag, N. Möller, A. Rühling, C. A. Strassert, B. J. Ravoo and F. Glorius, *ChemPhotoChem*, 2019, **3**, 24.
- 7 H. Bartling, A. Eisenhofer, B. König and R. M. Gschwind, *J. Am. Chem. Soc.*, 2016, **138**, 11860.
- 8 E. B. Corcoran, J. P. McMullen, F. Lévesque, M. K. Wismer and J. R. Naber, *Angew. Chem., Int. Ed.*, 2020, **59**, 11964.
- 9 (a) B. F. Buksh, S. D. Knutson, J. V. Oakley, N. B. Bissonnette, D. G. Oblinsky, M. P. Schwoerer, C. P. Seath, J. B. Geri, F. P. Rodriguez-Rivera, D. L. Parker, G. D. Scholes, A. Ploss and D. W. C. MacMillan, *J. Am. Chem. Soc.*, 2022, **144**(14), 6154; (b) S. Mallidi, S. Anbil, A.-L. Bulin, G. Obaid, M. Ichikawa and T. Hasan, *Theranostics*, 2016, **6**, 2458; (c) A. M. Smith, M. C. Mancini and S. Nie, *Nat. Nanotechnol.*, 2009, **4**, 710; (d) K. Szacilowski, W. Macyk, A. Drzewiecka-Matuszek, M. Brindell and G. Stochel, *Chem. Rev.*, 2005, **105**, 2647.
- 10 N. Sellet, M. Cormier and J.-P. Goddard, *Org. Chem. Front.*, 2021, **8**, 6783.
- 11 (a) D. C. Cabanero, J. A. Nguyen, C. S. Cazin, S. P. Nolan and T. Rovis, *ACS Catal.*, 2023, **13**, 4384; (b) N. Eng Soon Tay, K. Ah Ryu, J. L. Weber, A. K. Olow, D. C. Cabanero, D. R. Reichman, R. C. Oslund, O. O. Fadeyl and T. Rovis, *Nat. Chem.*, 2023, **15**, 101; (c) S. L. Goldschmid, N. Eng Soon Tay, C. L. Joe, B. C. Lainhart, T. C. Sherwood, E. M. Simmons, M. Sezen-Edmonds and T. Rovis, *J. Am. Chem. Soc.*, 2022, **144**, 22409; (d) S. L. Goldschmid, E. Bednarova, L. R. Beck, K. Xie, N. E. S. Tay, B. D. Ravetz, J. Li and C. L. Joe, *Synlett*, 2022, **33**, 247; (e) I. M. Ogbu, D. M. Bassani, F. Robert and Y. Landais, *Chem. Commun.*, 2022, **58**, 8802; (f) B. D. Ravetz, N. E. S. Tay, C. L. Joe, M. Sezen-Edmonds, M. A. Schmidt, Y. Tan, J. M. Janey, M. D. Eastgate and T. Rovis, *ACS Cent. Sci.*, 2020, **6**, 2053.
- 12 (a) C. Grundke, R. C. Silva, W. R. Kitzmann, K. Heinze, K. T. de Oliveira and T. Opitz, *J. Org. Chem.*, 2022, **87**, 5630; (b) Y. Katsurayama, Y. Ikabata, H. Maeda, M. Segi, H. Nakai and T. Furuyama, *Chem.-Eur. J.*, 2022, **28**, e202103223.
- 13 G. Han, G. Li, J. Huang, C. Han, C. Turro and Y. Sun, *Nat. Commun.*, 2022, **13**, 2288.
- 14 C. Ng, Z. Wu, T. Zhang, A. Phong Dang, Y. Yao, A. R. J. Nelson, S. W. Prescott, A. Postma, G. Moad, C. J. Hawker and C. Boyer, *Macromolecules*, 2023, **56**, 7898.
- 15 J. Sun, S. Ren, H. Zhao, S. Zhang, X. Xu, L. Zhang and E. Cheng, *ACS Macro Lett.*, 2023, **12**, 165.
- 16 N. Corrigan, J. Xu and C. Boyer, *Macromolecules*, 2016, **49**, 3274.
- 17 S. Shanmugam, J. Xu and C. Boyer, *Angew. Chem., Int. Ed.*, 2016, **55**, 1036.
- 18 A. Bonardi, F. Bonardi, G. Noirbent, F. Dumur, C. Dietlin, D. Gigmes, J.-P. Fouassier and J. Lalevée, *Polym. Chem.*, 2019, **10**, 6505.
- 19 N. Sellet, M. Sebbat, M. Elhabiri, M. Cormier and J.-P. Goddard, *Chem. Commun.*, 2022, **58**, 13759.
- 20 M. Tanioka, A. Kuromiya, R. Ueda, T. Obata, A. Muranaka, M. Uchiyama and S. Kamino, *Chem. Commun.*, 2022, **58**, 7825.
- 21 L. Zeng, Z. Wang, T. Zhang and C. Duan, *Molecules*, 2022, **27**, 4047.
- 22 B. K. Kundu, G. Han and Y. Sun, *J. Am. Chem. Soc.*, 2023, **145**, 3535.
- 23 G. S. Gopika, P. M. Hari Prasad, A. G. Lekshmi, S. Lekshmyapriya, S. Sreesaila, C. Arunima, M. S. Kumar, A. Anil, A. Sreekumar and Z. S. Pillai, *Mater. Today: Proc.*, 2021, **46**, 3102.
- 24 (a) K. Colas, S. Doloczki, M. Posada Urrutia and C. Dyrager, *Eur. J. Org. Chem.*, 2021, **15**, 2133; (b) L. Feng, W. Chen, X. Ma, S. H. Liu and J. Yin, *Org. Biomol. Chem.*, 2020, **18**, 9385.
- 25 C. Schwechheimer, F. Rönicke, U. Shepers and H.-A. Wagenknecht, *Chem. Sci.*, 2018, **9**, 6587.
- 26 S. S. Matikonda, D. A. Helmerich, M. Meub, G. Beliu, P. Kollmannsberger, A. Greer, M. Sauer and M. J. Schnermann, *ACS Cent. Sci.*, 2021, **7**, 1144.
- 27 J. N. Gayton, S. Autry, R. C. Fortenberry, N. I. Hammer and J. H. Delcamp, *Molecules*, 2018, **23**, 3051.
- 28 J. L. Bricks, Y. L. Slominskii, I. D. Panas and A. P. Demchenko, *Methods Appl. Fluoresc.*, 2018, **6**, 012001.



29 C. Sun, B. Li, M. Zhao, S. Wang, Z. Lei, L. Lu, H. Zhang, L. Feng, C. Dou, D. Yin, H. Xu, Y. Chen and F. Zhang, *J. Am. Chem. Soc.*, 2019, **141**, 19221.

30 (a) A. V. Kulinich, N. A. Derevyanko, A. A. Ishchenko, N. B. Gusyak, I. M. Kobasa, P. P. Romanczyk and S. S. Kurek, *Dyes Pigm.*, 2019, **161**, 24; (b) J. R. Lenhard and B. R. Hein, *J. Phys. Chem.*, 1996, **100**, 17287; (c) C. Chen, B. Zhou, D. Lu and G. Xu, *J. Photochem. Photobiol. A*, 1995, **89**, 25; (d) J. R. Lenhard and A. D. Cameron, *J. Phys. Chem.*, 1993, **97**, 4916; (e) T. Tani, *J. Electrochem. Soc.*, 1973, **120**, 254.

31 (a) H. Li, H. Kim, F. Xu, J. Han, Q. Yao, J. Wang, K. Pu, X. Peng and J. Yoon, *Chem. Soc. Rev.*, 2022, **51**, 1795; (b) N. G. Medeiros, C. A. Braga, V. S. Camara, R. C. Duarte and F. S. Rodembusch, *Asian J. Org. Chem.*, 2022, **11**, e202200095; (c) P. J. Choi, T. I.-H. Park, E. Cooper, M. Dragunow, W. A. Denny and J. Jose, *Bioconjugate Chem.*, 2020, **31**, 1724; (d) A. P. Gorka, R. R. Nani and M. J. Schnermann, *Acc. Chem. Res.*, 2018, **51**, 3226; (e) W. Sun, S. Guo, C. Hu, J. Fan and X. Peng, *Chem. Rev.*, 2016, **116**, 7768; (f) A. P. Gorka, R. R. Nani and M. J. Schnermann, *Org. Biomol. Chem.*, 2015, **13**, 7584.

32 G. Della Pelle, A. D. Lopez, M. S. Fiol and N. Kostevsek, *Int. J. Mol. Sci.*, 2021, **22**, 6914.

33 K. Bilici, S. Cetin, E. Celikbas, H. Y. Acar and S. Kolemen, *Front. Chem.*, 2021, **9**, 707876.

34 S. M. Usama, S. Thavornpradit and K. Burgess, *ACS Appl. Bio Mater.*, 2018, **1**, 1195.

35 J. Sun, E. Feng, Y. Shao, F. Lv, Y. Wu, J. Tian, H. Sun and F. Song, *ChemBioChem*, 2022, **23**, e202200421.

36 X. Zhao, Q. Yao, S. Long, W. Chi, Y. Yang, D. Tan, X. Liu, H. Huang, W. Sun, J. Du, J. Fan and X. Peng, *J. Am. Chem. Soc.*, 2021, **143**, 12345.

37 L. Jiao, F. Song, J. Cui and X. Peng, *Chem. Commun.*, 2018, **54**, 9198.

38 (a) E. N. Bifari, P. Almeida and R. M. El-Shishtawy, *Mater. Today: Proc.*, 2023, **36**, 101337; (b) W. Ghann, H. Kang, E. Emerson, J. Oh, T. Chavez-Gil, F. Nesbitt, R. Williams and J. Uddin, *Inorg. Chim. Acta*, 2017, **467**, 123.

39 C. H. Greville Williams, *Earth Environ. Sci. Trans. R. Soc. Edinburgh*, 1857, **21**, 377.

40 F. M. Hamer, *Q. Rev., Chem. Soc.*, 1950, **4**, 327.

41 (a) M. Panigrahi, S. Dash, S. Patel and B. K. Mishra, *Tetrahedron*, 2012, **68**, 781; (b) D. S. Pisoni, L. Todeschini, A. C. A. Borges, C. L. Petzhold, F. S. Rdoembusch and L. F. Campo, *J. Org. Chem.*, 2014, **79**, 5511; (c) G. S. Gopika, P. M. Hari Prasad, A. G. Lekshmi, S. Lekshmypriya, S. Sreesaila, C. Arunima, M. S. Kumar, A. Anil, A. Sreekumar and Z. S. Pillai, *Mater. Today: Proc.*, 2021, **46**, 3102.

42 N. G. Medeiros, C. A. Braga, V. S. Câmara, R. C. Duarte and F. S. Rodembusch, *Asian J. Org. Chem.*, 2022, **11**, e202200095.

43 (a) M. Lopalco, E. N. Koini, J. K. Cho and M. Bradley, *Org. Biomol. Chem.*, 2009, **7**, 856; (b) S. J. Mason, J. L. Hake, J. Nairne, W. J. Cummins and S. Balasubramanian, *J. Org. Chem.*, 2005, **70**, 2939.

44 L. Stackova, P. Stacko and P. Klán, *J. Am. Chem. Soc.*, 2019, **141**, 7155.

45 (a) For review see: C. D. Vanderwal, *J. Org. Chem.*, 2011, **76**, 9555; (b) S. Kunugi, T. Okubo and N. Ise, *J. Am. Chem. Soc.*, 1976, **98**, 2282; (c) E. N. Marvell, G. Caple and I. Shahidi, *J. Am. Chem. Soc.*, 1970, **92**, 5641; (d) E. N. Marvell and I. Shahidi, *J. Am. Chem. Soc.*, 1970, **92**, 5646; (e) W. König and J. Prakt, *Chem.*, 1904, **69**, 105.

46 S. M. Usama, S. C. Marker, D.-H. Li, D. R. Caldwell, M. Stroet, N. L. Patel, A. G. Tebo, S. Hernot, J. D. Kalen and M. Schnermann, *J. Am. Chem. Soc.*, 2023, **145**, 14647.

47 Z. Hao, L. Hu, X. Wang, Y. Liu and S. Mo, *Org. Lett.*, 2023, **25**, 1078.

48 H. Lee, J. C. Mason and S. Achilefu, *J. Org. Chem.*, 2006, **71**, 7862.

49 H.-H. Johannes, W. Grahn, A. Reisner and P. G. Jones, *Tetrahedron Lett.*, 1995, **36**, 7225.

50 L. Strekowski, M. Lipowska and G. Patonay, *J. Org. Chem.*, 1992, **57**, 4578.

51 R. M. Exner, F. Cortezon-Tamarit and S. I. Pascu, *Angew. Chem., Int. Ed.*, 2021, **60**, 6230.

52 R. Gray, D. Walton, J. Bickerton, P. Richard and J. Heptinstall, *Dyes Pigm.*, 1998, **38**, 97.

53 R. J. Mellamby, J. I. Scott, I. Mair, A. Fernandez, L. Saul, J. Arlt, M. Moral and M. Vandrell, *Chem. Sci.*, 2018, **9**, 7261.

54 K. Xu, H. Chen, J. Tian, B. Ding, Y. Xie, M. Qiang and B. Tang, *Chem. Commun.*, 2011, **47**, 9468.

55 K. Mitra, C. E. Lyons and M. C. T. Hartman, *Angew. Chem., Int. Ed.*, 2018, **57**, 10263.

56 G. Moad and D. H. Solomon, *The Chemistry of Radical Polymerization*, Elsevier, 2006.

57 (a) C. Nacci, M. Schnied, D. Civita, E. Magnano, S. Nappini, I. Pis and L. Grill, *J. Phys. Chem. C*, 2021, **125**, 22554; (b) M. Kaur and A. K. Srivastava, *J. Macromol. Sci., Part C: Polym. Rev.*, 2006, **42**, 481.

58 For review: B. Strehmel, C. Schmitz, C. Kütahya, Y. Pang, A. Drewitz and H. Mustroph, *Beilstein J. Org. Chem.*, 2020, **16**, 415.

59 (a) X. He, Y. Shao, Y. Pang, J. Wang, M. Lui, Y. Xin and Y. Zou, *Polym. Chem.*, 2023, **14**, 1543; (b) Q. Wang, S. Popov, V. Strehmel, J. S. Gutmann and B. Strehmel, *Polym. Chem.*, 2023, **14**, 116; (c) H. Mokbel, G. Noirbent, D. Gigmes, F. Dumur and J. Lalevée, *Beilstein J. Org. Chem.*, 2021, **17**, 2067; (d) Q. Wang, S. Popov, A. Feilen, V. Strehmel and B. Strehmel, *Angew. Chem., Int. Ed.*, 2021, **60**, 26855; (e) Y. Pang, A. Shiraishi, D. Keil, S. Popov, V. Strehmel, H. Jiao, J. S. Gutmann, Y. Zou and B. Strehmel, *Angew. Chem., Int. Ed.*, 2021, **60**, 1465; (f) Y. Pang, H. Jiao, Y. Zou and B. Strehmel, *Polym. Chem.*, 2021, **12**, 5752; (g) A. Caron, F. Dumur and J. Lalevée, *J. Polym. Sci.*, 2020, **58**, 2134.

60 (a) B. Jedrzejewska, M. Pietrzak and Z. Rafinski, *Polymer*, 2011, **52**, 2110; (b) S. Chatterjee, P. Gottschalk, P. D. Davis and G. B. Schuster, *J. Am. Chem. Soc.*, 1988, **110**, 2326.

61 J. Kabatc, M. Zasada and J. Paczkowski, *J. Polym. Sci., Part A: Polym. Chem.*, 2007, **45**, 3626.

62 A. H. Bonardi, F. Dumur, T. M. Grant, G. Noirbent, D. Gigmes, B. H. Lessard, J.-P. Fouassier and J. Lalevée, *Macromolecules*, 2018, **51**, 1314.



63 A. H. Bonardi, F. Bonardi, F. Morlet-Savary, C. Dietlin, G. Noirbent, T. M. Grant, J.-P. Fouassier, F. Dumur, B. H. Lessard, F. Gigmes and J. Lalevée, *Macromolecules*, 2018, **51**, 8808.

64 C. Kütahya, Y. Yagci and B. Strehmel, *ChemPhotoChem*, 2019, **3**, 1180.

65 C. Kütahya, C. Schmitz, V. Strehmel, Y. Yagci and B. Strehmel, *Angew. Chem., Int. Ed.*, 2018, **57**, 7898.

66 A. R. Obah Kosso, N. Sellet, A. Baralle, M. Cormier and J.-P. Goddard, *Chem. Sci.*, 2021, **12**, 6964.

67 Discussion about SET vs. EnT mechanisms for photocatalytic oxidation of amine: Y. Pan, S. Wang, C. W. Kee, E. Dubuisson, Y. Yang, K. P. Loh and C.-H. Tan, *Green Chem.*, 2011, **13**, 3341.

68 N. Sellet, L. Clement-Comoy, M. Elhabiri, M. Cormier and J.-P. Goddard, *Chem.-Eur. J.*, 2023, **29**, e202302353.

